ISSN 0965-5441, Petroleum Chemistry, 2023, Vol. 63, No. 7, pp. 759–768. © The Author(s), 2023. This article is an open access publication.
Russian Text © The Author(s), 2023, published in Sovremennye Molekulyarnye Sita. Advanced Molecular Sieves, 2023, Vol. 5, No. 2.

Microporous and Hierarchical ZSM-5 Zeolites in Friedländer Synthesis

N. G. Grigor'eva[a,*], S. V. Bubennov[a], A. S. Artem'eva[a], D. V. Serebrennikov[a], N. A. Filippova[a], and B. I. Kutepov[a]

[a] *Institute of Petrochemistry and Catalysis, Ufa Federal Research Center, Russian Academy of Sciences, Republic of Bashkortostan, Ufa, 450075 Russia*
**e-mail: ngg-ink@mail.ru*

Received July 20, 2023; revised August 14, 2023; accepted August 16, 2023

Abstract—The study investigates the catalytic performance of microporous and granular micro–meso–macroporous zeolites (H-ZSM-5 and H-ZSM-5h, respectively) in synthesis of quinolines by the reaction of 2-aminoacetophenone with diketones (2,4-pentanedione or dimedone), known as the Friedländer synthesis. In the presence of H-ZSM-5h, 1-(2,4-dimethylquinolin-3-yl)ethanone (**1a**) and 3,4-dihydro-3,3,9-trimethyl-1(2*H*)-acridinone (**1b**) were produced in 82 and 93% yields, respectively.

Keywords: Friedländer synthesis, zeolites, granular hierarchical zeolites, quinolines, acridinones

DOI: 10.1134/S0965544123050092

In recent years, researchers have paid increasing attention to the development of methods for producing organic chemicals in the presence of heterogeneous catalysts. Among organic chemicals synthesized over heterogeneous catalysts, of particular importance are quinolines, compounds extensively used to prepare bioactive pharmaceuticals [1], corrosion inhibitors [2], dyes [3], organic LEDs [4], and other chemicals. One of the best known techniques for the synthesis of quinolines and their derivatives is the Friedländer synthesis [5–7], a reaction that involves catalytic cyclocondensation of *o*-amino-substituted aromatic aldehydes, ketones, or their derivatives with substituted carbonyl compounds that contain active α-methylene groups [6]. Another example of *N*-heterocyclic compounds produced by the Friedländer reaction is the acridinone group, known for their antitubercular activity [8].

Previous research has described a variety of heterogeneous catalysts effective in the Friedländer synthesis, including supported acids (e.g., H_2SO_4/SiO_2 [9], phosphomolybdic acid/SiO_2 [10], and H_2SO_4/PEG [11]), SiO_2–Zn–MgO catalytic systems [12], oxide nanoparticles (e.g., oxides of copper [13], zinc [14], nickel [15], and titanium [16]), mesoporous silica gels SBA-15 with grafted Brønsted acid and base [17], and zeolites [18, 19].

MFI-type zeolites are among the most common industrial zeolites [20]. Two studies have reported on using microporous MFI zeolites in Friedländer synthesis [18, 19]. The research results were contradictory. López-Sanz et al. [18] report as low as 9% yield of quinolines over H-MFI. They explain this low activity by the channel sizes (0.53×0.56 and 0.51×0.55 nm) and, therefore, conclude that wide-pore zeolites or mesoporous materials are required to ensure adequate selectivity in the Friedländer synthesis of quinolines. In contrast, Teimouri and Najafi Chermahini [19] report up to 90% yield of quinolines in the presence of a microporous zeolite, specifically H-ZSM-5.

Microporous zeolites that have been researched are marked by rapid deactivation due to coking, leading to inadequate reagent conversion and promoting the formation of by-products. It would be fair to posit that the catalytic stability and selectivity towards desire secondary porosity levels (mesopores and macropores) into the microporous zeolite structure. To the best of our knowledge, catalytic systems of this kind have never been tested in Friedländer reactions.

This being so, it was of interest to investigate the Friedländer synthesis in the presence of a novel catalytic system based on granular H-ZSM-5h with a hierarchical porous structure [23]. This zeolite was synthesized in the Catalyst Preparation Laboratory of IPC UFRC RAS, in accordance with the procedure developed to prepare similar zeolites [24].

The H-Y_h and H-ZSM-5h granular hierarchical porous zeolites that we previously tested in synthesis of pyridines and quinolines by the Doebner–Miller and Skraup reactions exhibited higher performance than microporous zeolites of the identical structural type [23–27].

The present paper reports on an investigation of the catalytic performance of an H-ZSM-5h granular hierarchical (micro–meso–macroporous) zeolite in the reaction of 2-aminoacetophenone with acyclic and cyclic diketones (2,4-pentanedione and dimedone, respectively). The study results were compared with the data previously obtained in the presence of an H-ZSM-5 microporous zeolite.

EXPERIMENTAL

Reagents and catalysts. The following reagents were used for the Friedländer synthesis: 2-aminoacetophenone (>98%, Sigma-Aldrich) and diketones, specifically 2,4-pentanedione and 5,5-dimethyl-1,3-cyclohexanedione (dimedone, >99%, Acros). Toluene, acetone, D-chloroform, hexane, and ethyl acetate were used as solvents. The reagents were pre-treated in accordance with standard procedures [28].

A Na-ZSM-5h zeolite sample was synthesized in accordance with the procedure described in [22] from a powdered Na-ZSM-5 zeolite with a Si/Al molar ratio of 15 (manufactured by the Ishimbay Specialized Chemical Plant of Catalysts, Republic of Bashkortostan, Russia) and a specifically prepared amorphous aluminosilicate (Si/Al = 6). These components were mixed, wetted with water, granulated, and heat-treated at 550±5°C for 4 h, followed by hydrothermal crystallization in a sodium silicate solution.

H-zeolites were prepared by exchange of Na^+ cations for NH_4^+ followed by heat treatment in air at 550±5°C for 4–6 h. The Na^+/H^+ exchange degree amounted to 96–98%.

A $ZnCl_2$/H-ZSM-5h zeolite was prepared by capillary impregnation of the parent H-ZSM-5h sample with an alcoholic solution of $ZnCl_2$ (>97%, ACS reagent, manufactured by Acros). After the impregnation, the sample was held in a closed weighing cup for 16 h and under vacuum at 27°C for 2 h, then heat-treated in air at 450°C for 3 h. The nominal $ZnCl_2$ content was 6%.

Immediately prior to catalytic testing, the catalyst samples were calcined in air at 540°C for 3–4 h.

Characterization of catalysts. The chemical composition of the synthesized zeolites was identified by X-ray fluorescence (XRF) spectrometry using a Shimadzu EDX-7000P instrument.

The phase composition and crystallinity of the samples were characterized by X-ray diffraction (XRD) analysis on a Rigaku Ultima IV diffractometer in monochromated CuK_α radiation in the 2θ range of 3°–80° with a step of 0.5°/min. The zeolite crystallinity was evaluated as the ratio of the total integrated intensity of the crystalline phase to the sum of the total integrated intensities of the crystalline and amorphous phases. The XRD patterns were compared with the PDF2 database using PDXL software.

The specific surface area, micropore volume, and mesopore volume were measured by low-temperature (–196°C) nitrogen adsorption/desorption on a Nova 1200e sorption analyzer. Prior to testing, the samples were evacuated at 350°C for 6 h. The BET specific surface area was calculated at a relative partial pressure (P/P_0) of 0.2. The pore size distribution was derived from a BJH (Barrett–Joyner–Halenda) desorption curve, and the total pore volume was measured by the BJH method at P/P_0 = 0.95. The micropore volume in the presence of mesopores was estimated using Lippens and de Boer's *t*-Plot method [29].

The volume of macropores (at least 50 nm in size) was evaluated using a Carlo Erba Porosimeter 2000 mercury porosimeter. Prior to testing, the samples were evacuated at 25°C for 4 h.

The zeolite acidity was measured by IR spectroscopy of adsorbed pyridine. The IR spectra of adsorbed pyridine were recorded on a Bruker Vertex-70V FTIR spectrometer in the range of 400–4000 cm^{-1} with a resolution of 4 cm^{-1}. The samples were calcined *in vacuo* at 400°C for 4 h. The pellets for recording IR spectra were 15 mm in diameter. Pyridine adsorption was carried out at 150°C for 30 min, after which the physisorbed pyridine was removed by evacuation at 150°C for 30 min. Additionally, the pyridine was desorbed at 250 and 350°C for 30 min each. The Brønsted and Lewis acid sites (abbreviated as BAS and

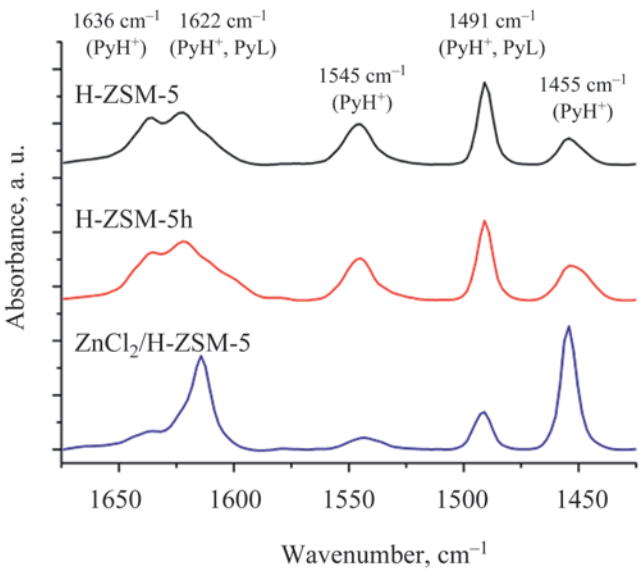

Fig. 1. IR spectra of adsorbed pyridine (at 150°C).

LAS, respectively) were quantified by peak integration at 1545 and 1450 cm^{-1}, respectively, based on the publicly reported integrated molar extinction coefficients of pyridine for both types of acid sites [30].

Catalytic test. 1-(2,4-Dimethylquinolin-3-yl)-ethanone (**1a**) was synthesized by a catalytic reaction between 2-aminoacetophenone and 2,4-pentanedione. The reaction was carried out in an autoclave at temperatures of 120–200°C, catalyst content of 5–35% (relative to the total reagent weight), and a ketoamine to 2,4-pentanedione molar ratio of 1 : 1.2. To synthesize 3,4-dihydro-3,3,9-trimethyl-1(2*H*)-acridinone (**1b**), a catalytic reaction between 2-aminoacetophenone and dimedone was carried out in an autoclave at 150°C, catalyst content of 20% (relative to the total reagent weight), and a ketoamine to dimedone molar ratio of 1 : 1.2. The autoclave was placed in an oven and heated under stirring for 5 h. After the reaction, the autoclave was cooled down, and the products were extracted from the reaction mixture with acetone. These products were then analyzed by a Crystallux 4000M gas chromatograph (GC) equipped with a thermal conductivity detector (TCD) and an Agilent DB-5 50 m×0.32 mm×0.52 μm glass capillary column (programmed heating from 100 to 250°C at a rate of 8°C/min, helium carrier gas). The conversion of the initial 2-aminoacetophenone was evaluated based on the toluene introduced as an internal standard in an amount of 10% of the initial ketoamine. Compounds (**1a**) and (**1b**) were separated by column chromatography (SiO_2, 100–200 mm) using a hexane/ethyl acetate (1 : 2) eluent mixture.

Mass spectra were recorded on a Shimadzu GCMS-QP2010 Plus gas chromatograph/mass spectrometer equipped with a SPB-5 30 m×0.25 mm capillary column (helium carrier gas, programmed heating from 40 to 300°C, ion source temperature 200°C, ionization energy 70 eV).

^1H and ^{13}C NMR, as well as COSY, HSQC, and HMBC (homo- and heteronuclear) spectra were recorded on a Bruker Avance III 500 HD Ascend instrument (500.17 MHz for ^1H nuclei and 125.78 MHz for ^{13}C nuclei, solvent $CDCl_3$).

RESULTS AND DISCUSSION

Physicochemical properties of zeolite catalysts. The physicochemical properties of the zeolite samples H-ZSM-5, H-ZSM-5h, and $ZnCl_2$/H-ZSM-5h are presented in Table 1. The properties of H-ZSM-5 and H-ZSM-5h were previously discussed in [23]. For $ZnCl_2$/H-ZSM-5h, both the specific surface area and pore volume were predictably lower than those for the parent H-ZSM-5h.

Figure 1 illustrates the IR spectra of adsorbed pyridine for the tested samples. The spectra display three absorption bands in the range of 1425–1575 cm^{-1}. The bands at 1455 cm^{-1} are typically attributed to pyridine adsorbed on LAS, and the bands at 1545 and 1636 cm^{-1}

Table 1. Physicochemical properties of catalysts[a]

Catalyst	Si/Al	β, %	S_{BET}, m^2/g	V_{micro}, cm^3/g	V_{meso}, cm^3/g	V_{macro}, cm^3/g	V_{total}, cm^3/g
H-ZSM-5	15	100	285	0.12	0.01	–	0.13
H-ZSM-5h	12	95–97	335	0.12	0.22	0.34	0.68
$ZnCl_2$/H-ZSM-5h	12	95–97	313	0.10	0.20	0.32	0.62

[a] β is the crystallinity; S_{BET} is the BET specific surface area; and V_{micro}, V_{meso}, V_{macro}, and V_{total} are the micropore, mesopore, macropore, and total pore volumes, respectively.

Table 2. BAS and LAS concentrations in zeolite samples based on IR spectra of adsorbed pyridine

Sample	Acid site concentration, μmol pyridine g^{-1}						BAS/ LAS[a]
	BAS			LAS			
	150°C	250°C	350°C	150°C	250°C	350°C	
H-ZSM-5	297	250	177	145	92	71	2.05
H-ZSM-5h	395	288	201	154	108	97	2.56
$ZnCl_2$/H-ZSM-5h	114	47	6	438	341	203	0.26

[a] BAS/LAS ratio evaluated for 150°C.

to protonated pyridine (BAS). The 1490 and 1622 cm^{-1} bands resulted from interaction between pyridine and all acid sites; moreover, the 1490 cm^{-1} signal was additionally caused by the appearance of hydrogen bonds [30].

The data presented in Table 2 show a BAS concentration in the H-ZSM-5h hierarchical zeolite that is about 1.3-fold higher than in the H-ZSM-5 microporous zeolite, and approximately equal LAS concentrations in both samples. The BAS/LAS ratios in H-ZSM-5 and H-ZSM-5h were 2.05 and 2.56, respectively. The incorporation of $ZnCl_2$ markedly lowered the BAS concentration (e.g., from 395 to 114 μmol pyridine g^{-1} at 150°C), with mostly remaining weak acid sites. The LAS concentration increased by a factor of 2.8 (from 154 to 438 μmol pyridine g^{-1}), with about half LAS being attributable to strong sites (203 μmol pyridine g^{-1}). The BAS/LAS ratio decreased to 0.26.

These data are consistent with a report published by Schmidt et al. [31]. In their study, after zeolite impregnation with $ZnCl_2$, zinc was present as large aggregates consisting of a ZnO/$ZnCl_2$ mixture and ion exchange particles –O–Zn–Cl. Thus, it is reasonable to associate the BAS concentration drop with partial ion exchange during the impregnation, and the LAS concentration rise by the presence of Lewis acids such as ZnO and $ZnCl_2$.

The catalytic performance of the H-ZSM-5-derived zeolite samples in the Friedländer synthesis was investigated for the case of cyclocondensation of 2-aminoacetophenone with various ketones such as 2,4-pentanedione and dimedone.

Cyclocondensation of 2-aminoacetophenone and 2,4-pentanedione occurs by the following route to produce 1-(2,4-dimethylquinolin-3-yl)ethanone (**1a**) (Scheme 1).

Table 3 presents the test data on the reaction between 2-aminoacetophenone and 2,4-pentanedione without a catalyst and in the presence of microporous (H-ZSM-5) and hierarchical zeolites (H-ZSM-5h and $ZnCl_2$/H-ZSM-5h).

It should be noted that the condensation of 2-aminoacetophenone with 2,4-pentanedione did not occur without a catalyst. In the presence of the tested catalysts, 1-(2,4-dimethylquinolin-3-yl)ethanone (**1a**) was the main reaction product. Minor concentrations of 2,4-dimethylquinoline (**2**), *N*-(2-acetylphenyl)acetamide (**3**), and products (denoted as "Others") of condensation of quinoline (**1a**) with the reagents were also detected in the reaction mixture. The hierarchical zeolite exhibited higher catalytic activity (in terms of aminoketone conversion)

Scheme 1. Reaction between 2-aminoacetophenone and 2,4-pentanedione.

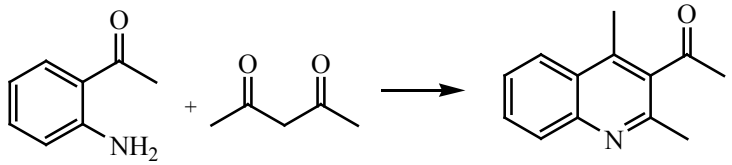

1a

Table 3. Reaction between 2-aminoacetophenone and 2,4-pentanedione[a]

Catalyst sample	2-aminoacetophenone conversion, %	Selectivity, %			
		1a	**2**	**3**	others
Catalyst-free	–	–	–		–
H-ZSM-5	45	88	4	7	1
H-ZSM-5h	55	98	1	1	0
$ZnCl_2$/H-ZSM-5h	71	79	6	12	3

[a] Reaction conditions: 20 wt % catalyst, ketoamine/2,4-pentanedione = 1 : 1.2 (mol), 5 h, 150°C; **1a** = (1-(2,4-dimethylquinolin-3-yl)-ethanone; **2** = 2,4-dimethylquinoline; and **3** = *N*-(2-acetylphenyl)acetamide.

and higher selectivity towards the desired quinoline (**1a**) than the mesoporous zeolite, which can be explained by a number of factors.

First of all, H-ZSM-5 and H-ZSM-5h differed in their acidic properties. Specifically, H-ZSM-5h was distinguished by a larger concentration and higher strength of BAS. Therefore, knowing that cyclocondensation occurs on strong acid sites [23, 24, 26, 32], it is reasonable to assume that this zeolite promoted cyclocondensation of amines with carbonyl compounds to produce a quinoline core. When strong acid sites are non-existent or deactivated, linear condensation reactions mostly take place.

Furthermore, the higher activity of H-ZSM-5h is associated with the presence of nanocrystals 15 to 100 nm in size [26], which shorten the diffusion path of reagents to active sites and that of products to the reaction media.

Finally, the greater accessibility of H-ZSM-5h active sites for reacting molecules was ensured by the presence of mesopores and macropores. Mesopores and macropores not only reduce diffusion problems for molecules but also encourage the formation of bulk molecules of the desired product, 0.60×0.91 nm in size (Fig. 2, ACD/3D Viewer).

When investigating the product composition in the reaction of 2-aminoacetophenone with 2,4-pentanedione, we detected two compounds that cannot be produced from Friedländer synthesis (Scheme 1), specifically 2,4-dimethylquinoline (**2**) and *N*-(2-acetylphenyl)-acetamide (**3**).

We assumed that these compounds could be produced by the following pathways (Scheme 2).

The reaction of 2-aminoacetophenone with 2,4-pentanedione may lead to Claisen-type C–C bond cleavage in the diketone molecule to form amide (**3**) and acetone (Scheme 2, reaction (1)). The newly-

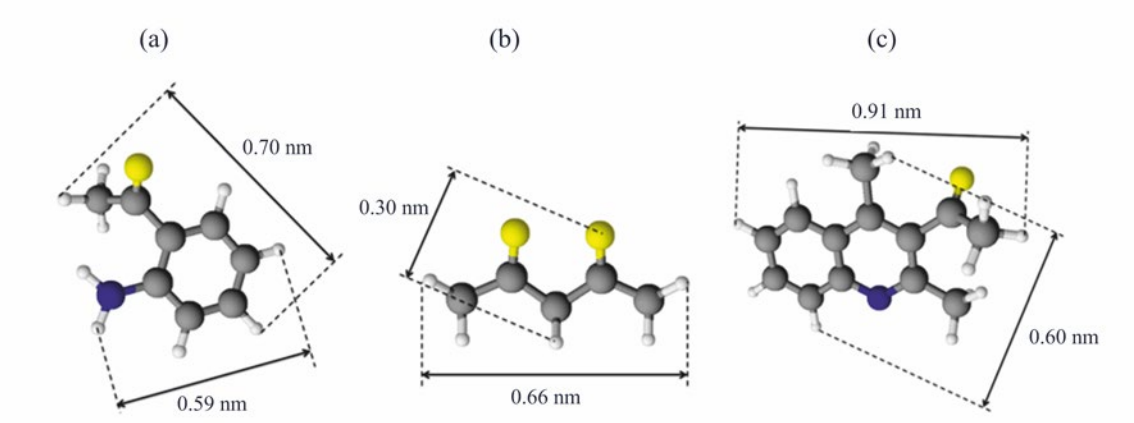

Fig. 2. Molecular size of reagents and reaction product: (a) 2-aminoacetophenone; (b) 2,4-pentanedione; and (c) (1-(2,4-dimethylquinoline-3-yl)ethanone (**1a**).

Scheme 2. Possible synthesis pathways of by-products.

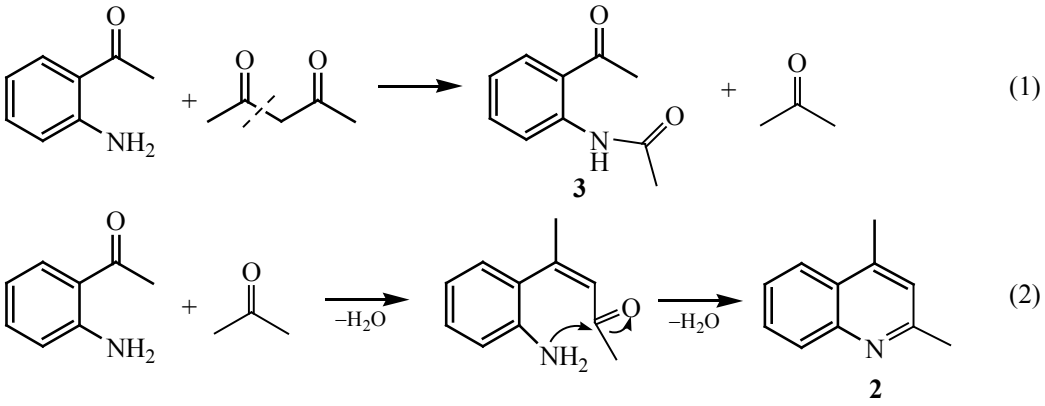

formed acetone enters into condensation with the 2-aminoacetophenone molecule followed by cyclization, to form dimethylquinoline (**2**) (Scheme 2, reaction (2)). Claisen reactions are known to involve LAS [33].

Given the presence of both BAS and LAS in the catalysts under study, it was safe to assume that these catalysts very likely promoted the reactions depicted in Scheme 2. To confirm this assumption, the H-ZSM-5h sample modified with a Lewis acid ($ZnCl_2$/H-ZSM-5h) was prepared. Table 3 presents the catalytic test data for this sample.

The data show that incorporating the additional Lewis acid enhanced the 2-aminoacetophenone conversion and the selectivity for amide (**3**) and quinoline (**2**), but the selectivity towards the desired quinoline (**1a**) declined from 98 to 79%. Therefore, the type of acid sites is critical to the occurrence of target reactions and to the suppression of side reactions in the zeolite-catalyzed Friedländer synthesis.

It is further worth noting that H-ZSM-5 exhibited higher selectivity towards by-products (**2, 3**) than H-ZSM-5h (see Table 3), which is likely due to the higher LAS concentration in H-ZSM-5 (33% in H-ZSM-5 vs 28% in H-ZSM-5h).

Thus, the higher activity and quinoline (**1a**) selectivity of H-ZSM-5h can be explained by its micro–meso–macroporous structure, nanocrystals, and high concentration of strong BAS.

Effects of reaction conditions. Figures 3 to 6 illustrate the test data on the effects of process temperature, catalyst content, and reaction time on the 2-aminoacetophenone conversion and product selectivity in the presence of H-ZSM-5h.

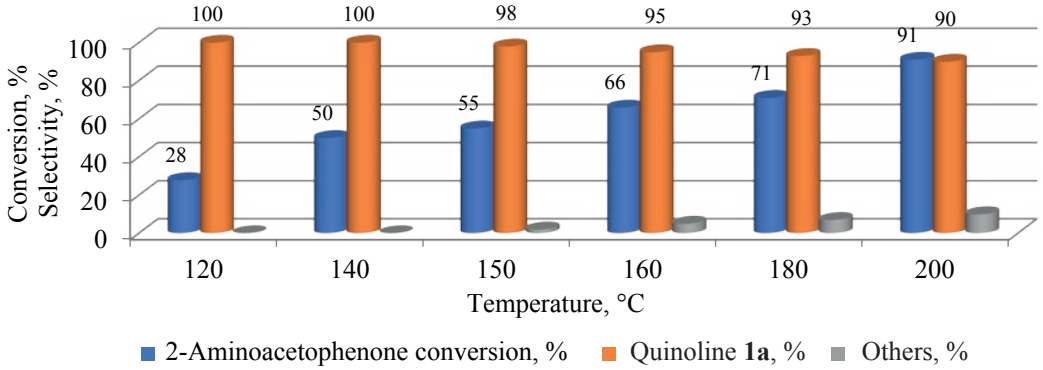

Fig. 3. Conversion of 2-aminoacetophenone and product selectivity as functions of temperature. Reaction conditions: autoclave, 20 wt % H-ZSM-5h, ketoamine/2,4-pentanedione = 1 : 1.2 (mol), 5 h.

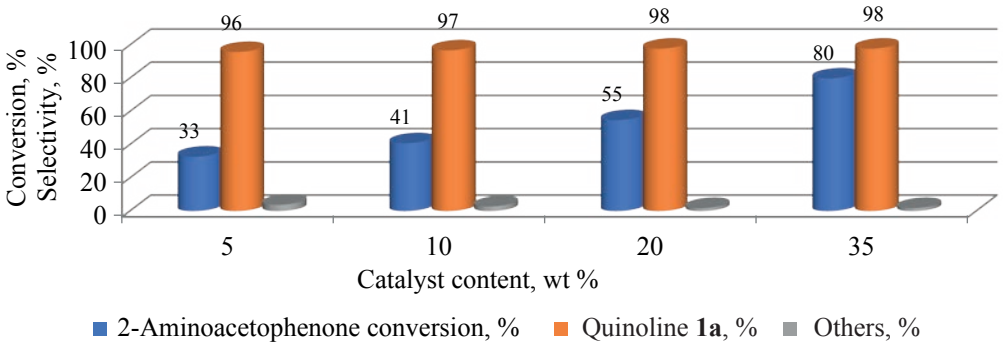

Fig. 4. Conversion of 2-aminoacetophenone and product selectivity as functions of catalyst content. Reaction conditions: autoclave, 150°C, H-ZSM-5h, ketoamine/2,4-pentanedione = 1 : 1.2 (mol), 5 h.

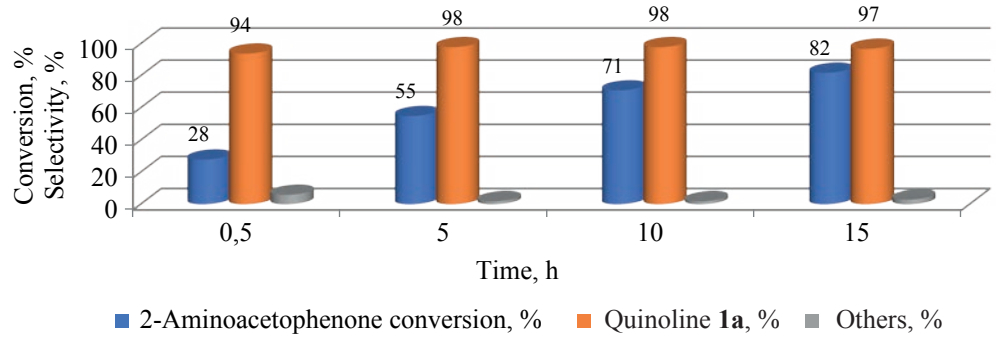

Fig. 5. Conversion of 2-aminoacetophenone and product selectivity as functions of reaction time. Reaction conditions: autoclave, 150°C, 20 wt % H-ZSM-5h, ketoamine/2,4-pentanedione = 1 : 1.2 (mol).

The highest quinoline (**1a**) selectivity (up to 100%) was achieved at 120–140°C, with 2-aminoacetophenone conversion of 28–50% (Fig. 3). Heating to 200°C increased the conversion to 91% and decreased the quinoline (**1a**) selectivity to 90%. Consequently, the diketone decomposition into acetone and subsequent synthesis of by-products (**2, 3**) took place on LAS at 150°C and higher temperatures. At lower temperatures (120–140°C), LAS are only involved in the target reaction. The highest yield of 1-(2,4-dimethylquinolin-3-yl)ethanone (**1a**), specifically 82%, was achieved at 200°C.

As the catalyst content ranged from 5 to 35 wt %, the quinoline selectivity varied insignificantly (from 96 to 98%), whereas the conversion increased by a factor of nearly 2.5 (Fig. 4).

To achieve a quinoline (**1a**) yield of 54% at 150°C, the reaction needed to occur for at least 5 h (Fig. 5). Further extension to 15 h enhanced the yield of the desired product to 80%. The quinoline (**1a**) selectivity remained almost unchanged.

Functional stability. The hierarchical porous structure of H-ZSM-5h not only enhances its catalytic activity and selectivity in the Friedländer synthesis but also favors its functional stability. Figure 6 illustrates the trends of 2-aminoacetophenone conversion and 1-(2,4-dimethylquinolin-3-yl)ethanone (**1a**) selectivity over four operating cycles of H-ZSM-5h and H-ZSM-5 without regeneration. Each cycle was carried out under the following conditions: 20 wt % catalyst, 150°C, 5 h, and ketoamine : 2,4-pentanedione = 1 : 1.2 (mol/mol).

It was found that after four cycles of H-ZSM-5h, the 2-aminoacetophenone conversion dropped from 55 to 40%, whereas the quinoline (**1a**) selectivity remained almost unchanged. In contrast, in the presence of the H-ZSM-5 microporous sample the conversion more than halved even after Cycle 2. The quinoline (**1a**) selectivity noticeably decreased after each operating cycle of H-ZSM-5.

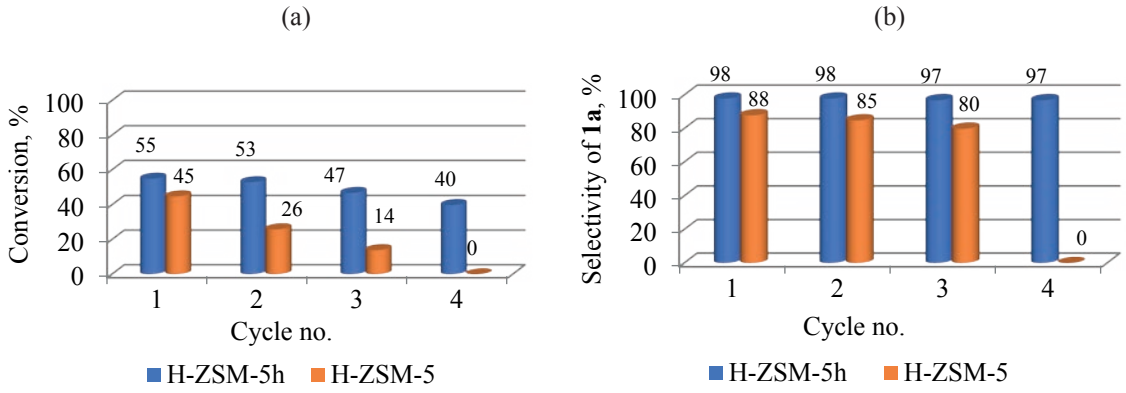

Fig. 6. Catalytic performance trends over four operating cycles: (a) 2-aminoacetophenone conversion; and (b) quinoline (**1a**) selectivity.

Scheme 3. Reaction of 2-aminoacetophenone with dimedone.

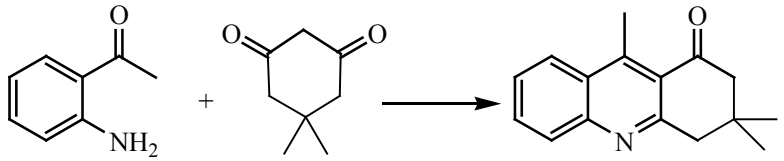

1b

To expand the potential of H-ZSM-5h in the Friedländer reaction, a quinoline derivative, specifically 3,4-dihydro-3,3,9-trimethyl-1(2*H*)-acridinone (**1b**) was synthesized by the reaction of 2-aminoacetophenone with dimedone (Scheme 3).

Under the reaction conditions imposed in the study (20 wt % catalyst, 150°C, ketoamine:dimedone = 1 : 1.2 mol/mol, 5 h), almost complete (99%) conversion of 2-aminoacetophenone was achieved, and 3,4-dihydro-3,3,9-trimethyl-1(2*H*)-acridinone (**1b**) was produced with 94% selectivity (93% yield). A comparative assessment of catalytic performance in the tested reactions demonstrated a higher yield of the desired product in the ketoamine reaction with cyclic diketone than with acyclic reagent.

CONCLUSIONS

The study investigated the catalytic performance of microporous and granular hierarchical micro–meso–macroporous zeolites (H-ZSM-5 and H-ZSM-5h, respectively) in synthesis of quinolines by the reaction of 2-aminoacetophenone with diketones (2,4-pentanedione or dimedone), known as the Friedländer synthesis. It was found that:

—In the reaction of 2-aminoacetophenone with 2,4-pentanedione, H-ZSM-5h exhibits higher catalytic activity (expressed as a ketoamine conversion of 55%), higher selectivity towards 1-(2,4-dimethylquinolin-3-yl)ethanone (**1a**, 98%), and higher functional stability than H-ZSM-5 (for which the ketoamine conversion and quinoline **1a** selectivity reached 45 and 88%, respectively). The higher performance of H-ZSM-5h can be explained by a combination of three critical factors: the high concentration of strong Brønsted acid sites, the micro–meso–macroporous structure, and the presence of nanocrystals;

—Increasing the concentration of Lewis acid sites in a zeolite catalyst leads to an increased selectivity towards by-products and a lowered yield of desired quinoline (**1a**);

—When testing the effects of process conditions (such as temperature, catalyst content, and reaction time) in the reaction of 2-aminoacetophenone with 2,4-pentanedione over H-ZSM-5h, the highest yield of quinoline (**1a**), specifically 82%, was achieved under the following conditions: 200°C, 20 wt % catalyst, ketoamine : 2,4-pentanedione = 1 : 1.2 mol/mol, 5 h; and

—In the presence of H-ZSM-5h, the reaction of 2-aminoacetophenone with cyclic diketone (dimedone)

provides a higher yield of the desired product (3,4-dihydro-3,3,9-trimethyl-1(2*H*)-acridinone, **1b**) than the reaction with acyclic diketone (2,4-pentanedione).

AUTHOR INFORMATION

N.G. Grigor'eva, ORCID: https://orcid.org/0000-0001-6451-9205

S.V. Bubennov, ORCID: https://orcid.org/0000-0002-2230-772X

A.S. Artem'eva, ORCID: https://orcid.org/0000-0001-7668-4929

D.V. Serebrennikov, ORCID: https://orcid.org/0000-0002-6601-390X

N.A. Filippova, ORCID: https://orcid.org/0000-0002-8994-3456

B.I. Kutepov, ORCID: https://orcid.org/0000-0003-0745-5510

FUNDING

This work was performed within the State Program of IPC UFRC RAS (project no. FMRS-2022-0080). The structural investigation was carried out at the Agidel Regional Center for Collective Use of UFRC RAS within the State Program of IPC UFRC RAS (project no. FMRS-2022-0081).

CONFLICT OF INTEREST

The authors declare no conflict of interest requiring disclosure in this article.

OPEN ACCESS

REFERENCES

1. Kumar, S., Bawa, S., and Gupta, H., *Mini-Rev. Med. Chem*., 2009, vol. 9, no. 14, pp. 1648–1654. https://doi.org/10.2174/138955709791012247
2. Lavanya, K., Saranya, J., and Chitra, S., *Corros. Rev*., 2018, vol. 36, no. 4, pp. 365–371. https://doi.org/10.1515/corrrev-2017-0129
3. Ilina, K. and Henary, M., *Chem. Eur. J*., 2021, vol. 27, no. 13, pp. 4230–4248. https://doi.org/10.1002/chem.202003697
4. Wang, S., Zhang, H., Zhang, B., Xie, Z., and Wong, W.-Y., *Mater. Sci. Eng.: R: Reports*, 2020, vol. 140, p. 100547. https://doi.org/10.1016/j.mser.2020.100547
5. Rajendran, S., Sivalingam, K., Karnam Jayarampillai, R.P., Wang, W., and Salas Cristian, O., *Chem. Biol. Drug. Des*., 2022, vol. 100, no. 6, pp. 1042–1085. https://doi.org/10.1111/cbdd.14044
6. Ghobadi, N., Nazari, N., and Gholamzadeh, P., *Adv. Heterocycl. Chem.*, 2020, vol. 132, pp. 85–134. https://doi.org/10.1016/bs.aihch.2020.01.001
7. Marco-Contelles, J., Pérez-Mayoral, E., Samadi, A., do Carreiras, M.C., and Soriano, E., *Chem. Rev*., 2009, vol. 109, no. 6, pp. 2652–2671. https://doi.org/10.1021/cr800482c
8. Gensicka-Kowalewska, M., Cholewiński, G., and Dzierzbicka, K., *RSC Adv.*, 2017, vol. 7, no. 26, pp. 15776–15804. https://doi.org/10.1039/C7RA01026E
9. Narasimhulu, M., Reddy, T.S., Mahesh, K.C., Prabhakar, P., Rao, Ch.B., and Venkateswarlu, Y., *J. Mol. Catal. A: Chemical*, 2007, vol. 266, nos. 1–2, pp. 114–117. https://doi.org/10.1016/j.molcata.2006.10.049
10. Das, B., Krishnaiah, M., Laxminarayana, K., and Nandankumar, D., *Chem. Pharm. Bull*., 2008, vol. 56, no. 7, pp. 1049–1051. https://doi.org/10.1248/cpb.56.1049
11. Zhang, X.-L., Wang, Q.-Y., Sheng, S.-R., Wang, Q., and Liu, X.-L., *Synth. Commun*., 2009, vol. 39, no. 18, pp. 3293–3304. https://doi.org/10.1080/00397910902754283
12. Brahmayya, M., Venkateswara Rao, B., Viplavaprasad, U., and Basaveswara Rao, M.V., *J. App. Pharm. Sci*., 2012, vol. 2, no. 10, pp. 41–44. https://doi.org/10.7324/JAPS.2012.21008
13. Nezhad, J.M., Akbari, J., Heydari, A., and Alirezapour, B., *Bull. Korean Chem. Soc*., 2011,

vol. 32, no. 11, pp. 3853–3854.
https://doi.org/10.5012/BKCS.2011.32.11.3853
14. Hosseini-Sarvari, M., *JICS*, 2011, vol. 8, suppl. 1, pp. 119–S128.
https://doi.org/10.1007/BF03254288
15. Angajala, G. and Subashini, R., *RSC Adv*., 2015, vol, no. 57, pp. 45599–45610.
https://doi.org/10.1039/C5RA06593C
16. Bandyopadhyay, P., Prasad, G.K., Sathe, M., Sharma, P., Kumar, A., and Kaushik, M.P., *RSC Adv*., 2014, vol. 4, no. 13, p. 6638.
https://doi.org/10.1039/c3ra46128a
17. Patent ES 2395109 (A1), 2013.
18. López-Sanz, J., Pérez-Mayoral, E., Procházková, D., Martín-Aranda, R.M., and López-Peinado, A.J., *Top. Catal.*, 2010, vol. 53, nos. 19–20, pp. 1430–1437.
https://doi.org/10.1007/s11244-010-9603-8
19. Teimouri, A. and Najafi Chermahini, A.A., *Arabian J. Chem*., 2016, no. 9, pp. 5433–5439.
https://doi.org/10.1016/j.arabjc.2011.05.018
20. Travkina, O.S., Agliullin, M.R., and Kutepov, B.I., *Katal. Prom–ti*, 2021, vol. 21, no. 5, pp. 297–307.
https://doi.org/10.18412/1816-0387-2021-5-297-307
21. Kutepov, B.I., Travkina, O.S., Agliullin, M.R., Khazipova, A.N., Pavlova, I.N., Bubennov, S.V., Kostyleva, S.A., and Grigor'eva, N.G., *Petrol. Chem*., 2019, vol. 59, no. 3, pp. 297–309.
https://doi.org/10.1134/S0965544119030095
22. Patent RU 2739350C1, 2022.
23. Grigorieva, N.G., Travkina, O.S., Bubennov, S.V., Filippova, N.A., Artem'eva, A.S., Bayburtli, A.V., Kuvatova, R.Z., and Kutepov, B.I., *Kinet. Catal*., 2022, vol. 63, no. 6, pp. 781–792.
https://doi.org/10.1134/S0023158422060052
24. Grigor'eva, N.G., Kostyleva, S.A., Artem'eva, A.S., Bubennov, S.V., and Kutepov, B.I., *Petrol. Chem*., 2020, vol. 60, no. 4, pp. 525–531.
https://doi.org/10.1134/S0965544120040088
25. Grigor'eva, N.G., Bayburtli, A.V., Kuvatova, R.Z., Semenova, T.V., Bubennov, S.V., Raskildina, G.Z., Zlotsky, S.S., and Kutepov, B.I., *Russ. Chem. Bull*., 2020, vol. 69, no. 3, pp. 525–528.
https://doi.org/10.1007/s11172-020-2793-8
26. Grigorieva, N.G., Bayburtli, A.V., Travkina, O.S., Bubennov, S.V., Kuvatova, R.Z., Artem'eva, A.S., and Kutepov, B.I., *ChemistrySelect*, 2022, vol. 7, pp. 1–9.
https://doi.org/10.1002/slct.202103532
27. Bayburtli, A.V., Grigorieva, N.G., Raskil'dina, G.Z., Zlotsky, S.S., and Kutepov, B.I., *Doklady Chem*., 2020, no. 490(2), pp. 32–35.
https://doi.org/10.1134/S0012500820020019
28. Gordon, A.J. and Ford, R.A., *The Chemist's Companion: A Handbook of Practical Data, Techniques, and References*, Wiley, 1972.
29. Gregg, S.J. and Sing, K.S., *Adsorption, Surface Area, and Porosity*, London.: Academic Press, 1995.
30. Tamura, M., Shimizu, K., and Satsuma, A., *Appl. Catal. A: General*, 2012, vols. 433–434, pp. 135–145.
https://doi.org/10.1016/j.apcata.2012.05.008.
31. Schmidt, S.A., Kumar, N., Shchukarev, A., Eränen, K., Mikkola, J.-P., Murzin, D.Yu., and Salmi, T., *Appl. Catal. A: General*, 2013, vol. 468, pp. 120–134.
https://doi.org/10.1016/j.apcata.2013.08.039
32. Huang, C., Li, A., Li, L.-J., and Chao, Z.-S., *RSC Adv*., 2017, vol. 7, no. 40, pp. 24950–24962.
https://doi.org/10.1039/C7RA04526C
33. Hussein, M.A., Huynh, V.T., Hommelsheim, R., Koenigs, R.M., and Nguyen, T.V., *Catalyst. Chem. Commun*., 2018, vol. 54, no. 92, pp. 12970–12973.
https://doi.org/10.1039/C8CC07329E